COMPUTATIONAL ANALYSIS OF NOISE GENERATION AND PROPAGATION MECHANISMS USING THE EXAMPLE OF AN HVAC BLOWER

Barbara NEUHIERL[1], Attila FELFÖLDI[1]

[1] *EXA GmbH, Landshuter Allee 8, 80637 München, Germany*

SUMMARY

This paper describes a computational approach to simulate passenger car HVAC blower noise. The Lattice-Boltzmann Method (LBM) is used to simulate both flow and acoustics at the same time. The blower to be examined is placed in an idealized environment, consisting of a settling box in an anechoic room. To also take into account a more realistic situation, an air intake – a original part typically mounted in vehicles - was added. It is demonstrated how the mounting conditions can affect the flow and thus the noise generation. Besides validation by comparison to experiments, the purpose of the study is in the first place to analyze and visualize flow structures influencing noise generation.

INTRODUCTION

In general, in early product development phases, fans and blowers are typically evaluated within a substitute system in experiment, without the HVAC system or cooling package, but mounted in a test environment instead. Nevertheless the crucial mechanisms leading to noise generation and affecting the fan or blower performance must be represented. Thus it is a goal to create boundary conditions in experiment as realistic as possible.

The test environment used for the examinations discussed in this paper consists of a settling box placed inside a semi-anechoic chamber with an imposed mass flow. The rotating blower is mounted at an opening. Outside the box, within the anechoic environment, microphones are positioned.

One great advantage of CFD (Computational Fluid Dynamics) lies in the possibility to evaluate systems in early phases without the existence of a physical prototype and furthermore gather insight into mechanisms and flow behavior that is expensive and time consuming or not possible at all with experiments only.

The experiment can indeed give overall results, like e.g. sound pressure measured in different microphone positions, showing general differences and enabling the comparison of different

designs in terms of the noise generated, requiring a physical prototype for each variation. By testing virtually, the number of prototypes can be reduced significantly.

In order to validate the approach, CFD microphone results were compared to experiments and showed good correlation.

Analyzing in detail the flow properties inside the system that can lead to the generation of sound is costly if not impossible at all. So, another advantage of simulation is the possibility to gain more insight into the flow. Detailed analysis both in time and frequency domain are done typically to analyze and understand better the noise generation and propagation mechanisms.

Special focus was set on examining influence of more real conditions. To achive this, another configuration with an additional inlet grid was investigated which was supposed to lead to a disturbed thus more realistic flow.

In order to avoid a two-step approach where first a fluid simulation is performed and then e.g. acoustic analogies are used to predict sources for a standalone acoustic propagation simulation, the Lattice-Boltzmann method, a kinetic scheme modeling the dynamics of particle distributions, was used in combination with rotating meshes representing the blower movement. This allows the prediction of both transient hydrodynamic flow structures as well as the generation and propagation of acoustic waves within the fluid at the same time.

COMPUTATIONAL FLUID DYNAMICS WITH THE LATTICE-BOLTZMANN-METHOD

Lattice-Boltzmann-Method

The simulations were performed using EXA PowerFlow, a CFD code based on the Lattice-Boltzmann-Method (see [1]-[4]).

Most of the conventional CFD methods solve the *macroscopic* Navier-Stokes equations – a system of partial differential equations describing the continuum.

The Lattice-Boltzmann method on the other side is based on a *mesoscopic* kinetic equation for the particle distribution function. The respective macroscopic transient fluid behaviour evolves from the particle distributions in time. The Lattice-Boltzmann equation has the following form:

$$f_i(\vec{x}+c_i,t+\Delta t)-f_i(\vec{x},t)=C_i(\vec{x},t) \qquad (1)$$

f_i is the particle distribution function which moves according to a finite set of discrete velocity vectors $\{c_i: i=0,\ldots,b\}$ in the direction of i. c_i Δt und Δt are the respective spatial and time increments. Here $\Delta t = 1$ is assumed.

The right side of equation (1) consists of the so-called collision operator C_i. It determines whether the fluid behavior is physical, e.g. if the necessary conservation laws are satisfied.

The most popular formulation is the Bhatnagar-Gross-Krook (BGK)-form (see [5], [6]):

$$C_i(\vec{x},t)=-\frac{1}{\tau}\left[f_i(\vec{x},t)-f_i^{eq}(\vec{x},t)\right] \qquad (2)$$

τ represents a time relaxation parameter and f_i^{eq} a local equilibrium distribution function dependent of local hydrodynamic properties.

Macroscopic direct and derived fluid variables (density, pressure, velocity, momentum) can be obtained by summarizing the particle distributions, e.g.:

$$\rho(\vec{x},t)=\sum_i f_i(\vec{x},t),\ \ \rho\vec{u}(\vec{x},t)=\sum_i c_i f_i(\vec{x},t) \tag{3}$$

In the case of low frequencies and wave numbers and for suitable discrete velocity vectors and small mach numbers (Mach < 0.5), the Navier-Stokes equations can be derived from the Lattice-Boltzmann equation by performing the so-called Chapman-Enskog expansion. The resulting equation of state obeys the ideal gas law, and the kinematic viscosity is related to the relaxation parameter τ and temperature T (see [7], [8]):

$$\nu=(\tau-\frac{1}{2})T \tag{4}$$

Equations (2) to (4) represent a typical Lattice-Boltzmann scheme. It is resolved on a regular carthesian grid. The code enables local grid refinement, thus the resolution can be adapted to the simulated problem.

Turbulence Model

In order to model also small fluctuations in the flow field not resolved by the grid, the Lattice-Boltzmannn equation is extended by replacing the molecular by a turbulent relaxation time scale: $\tau \rightarrow \tau_{eff}$. τ_{eff} is formulated by a RNG (Renormalization Group) prodecure (see [9]). Such a simulation is called *Very-Large-Eddy-Simulation* (VLES) (see [10] - [12]).

To be able to take into account the typically high-Reynolds number small boundary layers, a turbulent wall model is implemented, approximating the respective boundary conditions (see [13]).

Rotating Geometry

Simulations that contain arbitrary shaped rotating geometry, like blowers or fans, require that the simulation domain is divided into an inner so-called Local Reference Frame (LRF) domain covering the parts rotating around a fixed axis, and an outer “ground-fixed” reference frame domain, covering the non-moving parts.
Details related to the implementation of rotation geometry and the interface region can be found in [14], [15].

Benefits of the Chosen Numerical Approach

The Lattice-Boltzmann method hence simulates very efficiently transient, compressible fluid flows, meeting the requirement of representing both the flow and the acoustic field that is generated by the flow and at the same time propagating within the fluid. Consequently there is no need to apply acoustic analogies where noise sources are determined from flow parameters and the acoustic propagation is then calculated separately afterwards. Flow and acoustics are calculated by a one-field simulation instead. Possible interactions between flow structures and acoustic field are represented inherently.

TEST ENVIRONMENT AND SIMULATION MODEL

Base Configuration

Experiments were performed in a semi-anechoic room with acoustically absorbing walls and a reverberant floor. Inside this room a so-called settling box was placed. It consists of a closed cavity where the walls are lined with absorbing material. A constant mass flow is imposed via an inlet equipped with mufflers to dampen out background noise. A typical HVAC blower is mounted inside the box, as shown in picture 1, on a cantilever arm. It is connected via a duct to an opening in the wall of the box, thus blowing into the anechoic environment.

Figure 1: Foto of blower mounted inside the settling box (left), simulation model of settling box with absorbing material and blower geometry (right)

The simulation model was built accordingly to the test environment. To represent the anechoic walls of the test chamber, layers with increased viscosity were assumed. This leads to a free-field radiation condition. To take into account reflections, a reverberant floor was modelled which had the same distance to the test object as in reality.

The finest resolution of the flow domain was chosen to be 0.4 mm around the blower wheel.

In the experiment, a microphone was positioned in 1 meter relative distance to the opening of the settling box, but outside the air flow. For comparison reasons, in the simulation, a probe position was defined at the same position, and pressure was recorded over time.

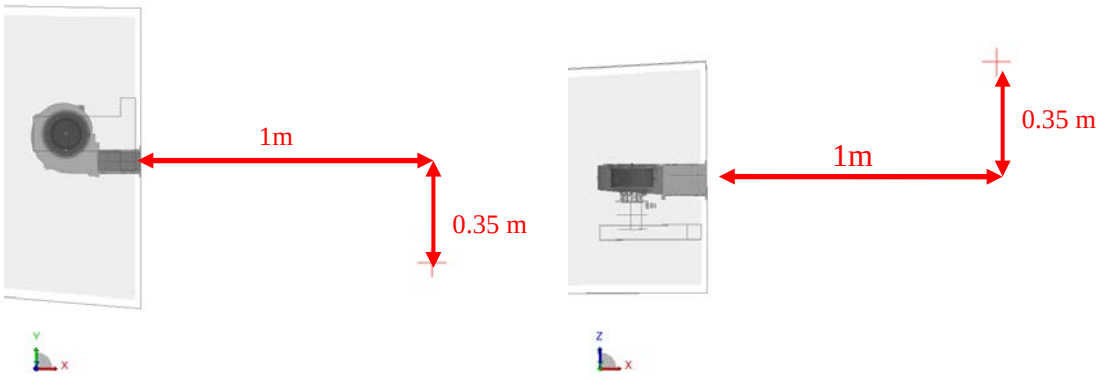

Figure 2: Microphone position relative to settling box opening

Variation

Both in simulation and experiment, in order to investigate more realistic flow conditions, an air intake was mounted above the blower. This is a part that is present typically in "real" environments at the intake area of an HVAC system. It has two openings, one for "outside air" (OSA) operating mode, where the air is ingressing from the environment, and another one for "recirculation" mode where the air is drawn in from the passenger cabin. The outside air inlet door was closed (see Figure 3 below).

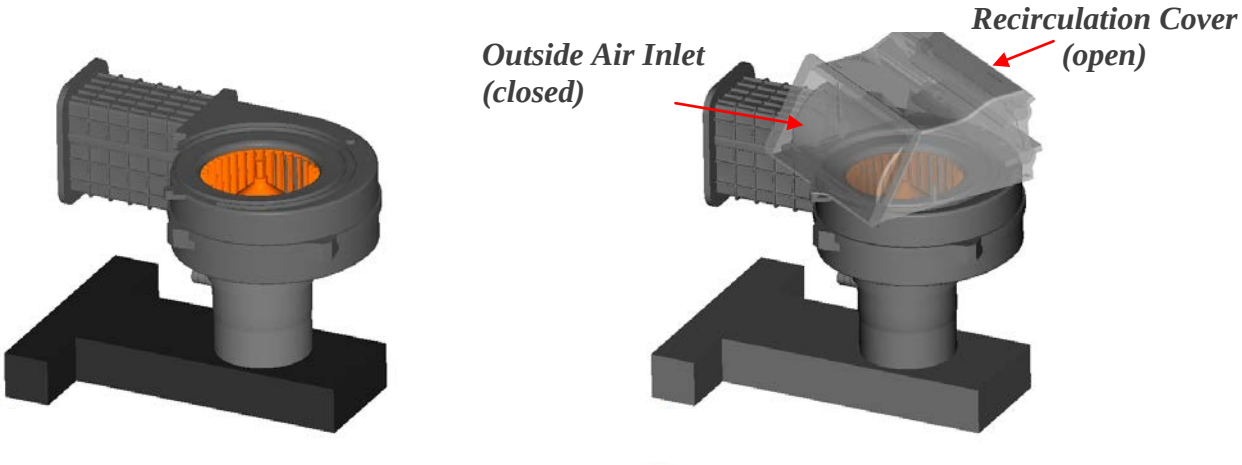

Figure 3: Base configuration: Blower with undisturbed inlet area (left);
Variant: air intake mounted above blower (right)

RESULTS

Validation by comparing simulation and experiment

The comparison of test and simulation results shows reasonable correlation for both configurations, see Figure 4.

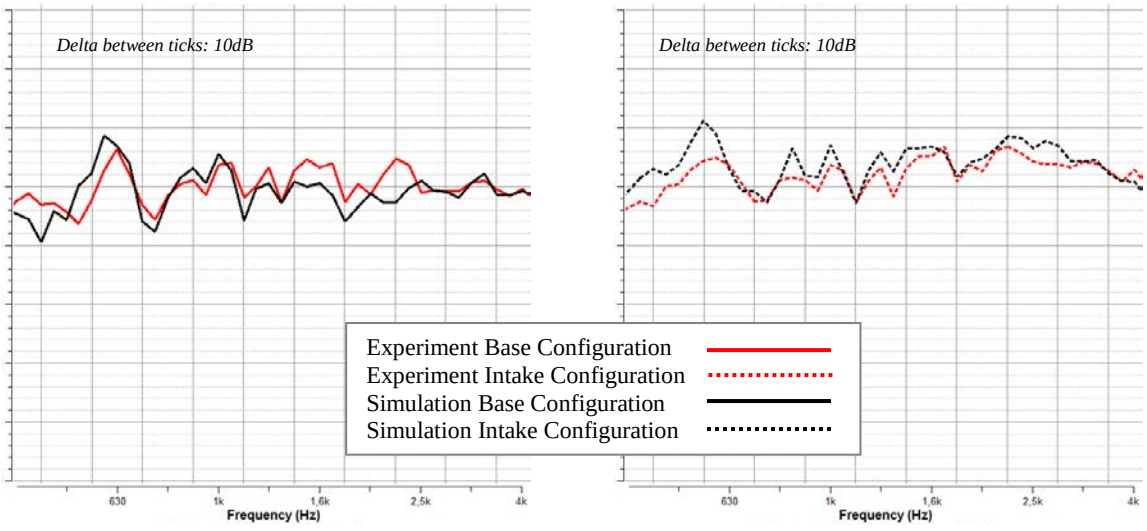

Figure 4: Sound pressure level (dBA) for both configurations at microphone location, experiment (red curves) versus simulation (black curves), 12th octave band

This – together with the fact that the pressure rise predicted by the simulation was 2 % accurate – gives confidence that the simulation leads to fairly realistic assessment of the flow and acoustics.

In Figure 5 on the right hand side the curves for both experiments – the blower with and without intake – are compared, while the left hand side shows the same comparison for the simulation results. Differences between the two configurations can be observed for frequencies > 1 kHz (indicated by the dashed yellow circle in Figure 5) and around 500 -630 Hz (indicated by the dashed green circle in Figure 5) where the case with intake is clearly louder. Both simulation and experiment show the same trend.

(The fact that the simulation gives a higher absolute increase can be explained e.g. by uncertainties in the modelling of the settling box interior, especially the acoustic liner whose properties were estimated).

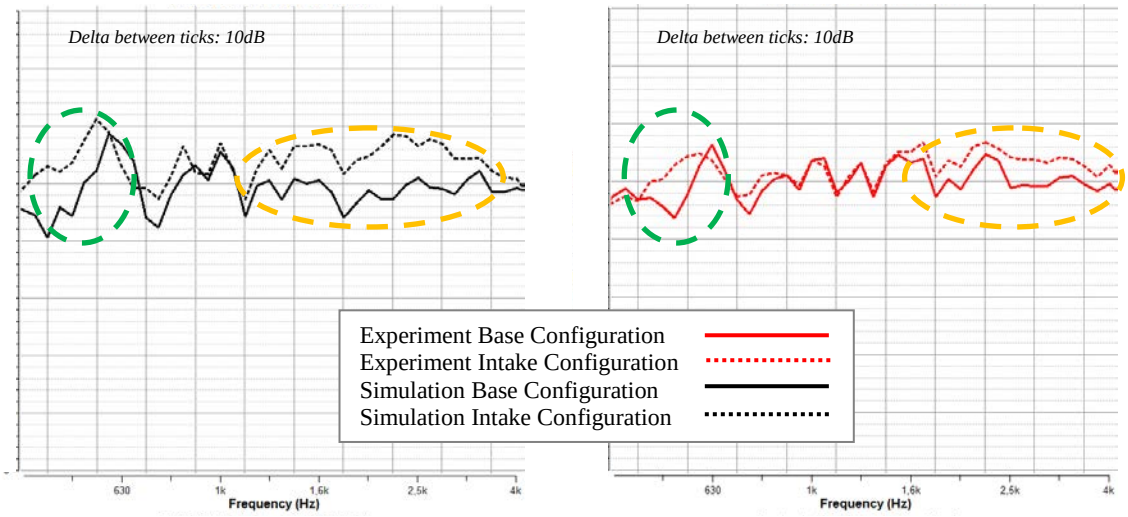

Figure 5: Sound pressure level (dBA) at microphone location, simulation (black curves, left) versus experiment (red curves, right),each with base and intake configuration, 12th octave band

Simulation results

This chapter describes selected flow structures around and through the blower and how they are influenced by additional geometry, here the air intake.

Figure 6 shows instantaneous velocity magnitude in a plane cutting through the blower wheel. The case on the left hand side without the air intake has “ideal” inlet conditions, while the picture on the right demonstrates clearly to what extent the ingress flow is disturbed.

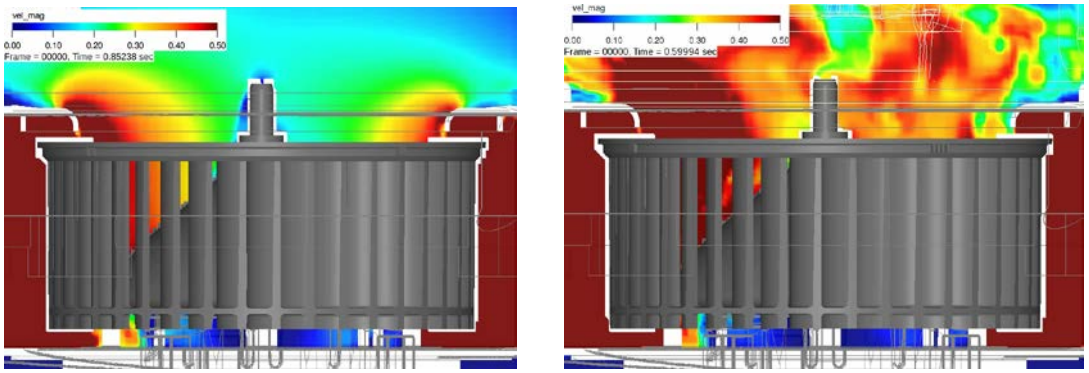

Figure 6: Instantaneous transient velocity magnitude (made dimensionless by dividing by blower tip velocity) on plane cutting vertically through the blower wheel:
incoming flow is affected by air intake

Figure 7 also displays instantaneous velocity magnitude, but this time on a horizontal plane cutting through the wheel and also through the outlet duct. Higher velocities can be observed locally, close to the wheel blades for the case with air intake. As the wheel itself has the same angular velocity implied, the increase in velocity must be owed to the narrower inlet path.

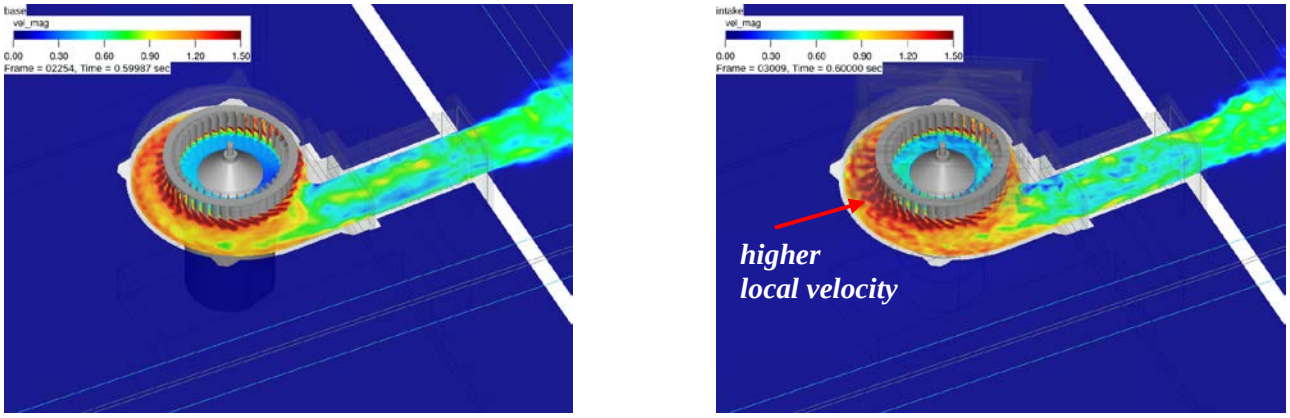

Figure 7: Instantaneous transient velocity magnitude (made dimensionless by dividing by blower tip velocity) on horizontal plane cutting through the wheel and outlet duct

Regions where high transient velocities occur together with strong vortex structures are often causing the generation of acoustic sources. With Lambda 2 (which is the 2nd largest eigenvalue of $S_{ij}^2+\Omega_{ij}^2$, see equation (5))

$$S_{ij}^2+\Omega_{ij}^2 \quad with: \quad S_{ij}=\frac{1}{2}\left(\frac{\partial v_i}{\partial x_j}+\frac{\partial v_j}{\partial x_i}\right) \quad and \quad \Omega_{ij}=\frac{1}{2}\left(\frac{\partial v_i}{\partial x_j}-\frac{\partial v_j}{\partial x_i}\right) \tag{5}$$

isosurfaces as a criterium for vortices, it can be shown that of course a lot of turbulent structures seem to be caused by the flow that is going over the door insets of the air intakes' opening (see red arrow in Figure 8, and zoom-in picture in Figure 9).

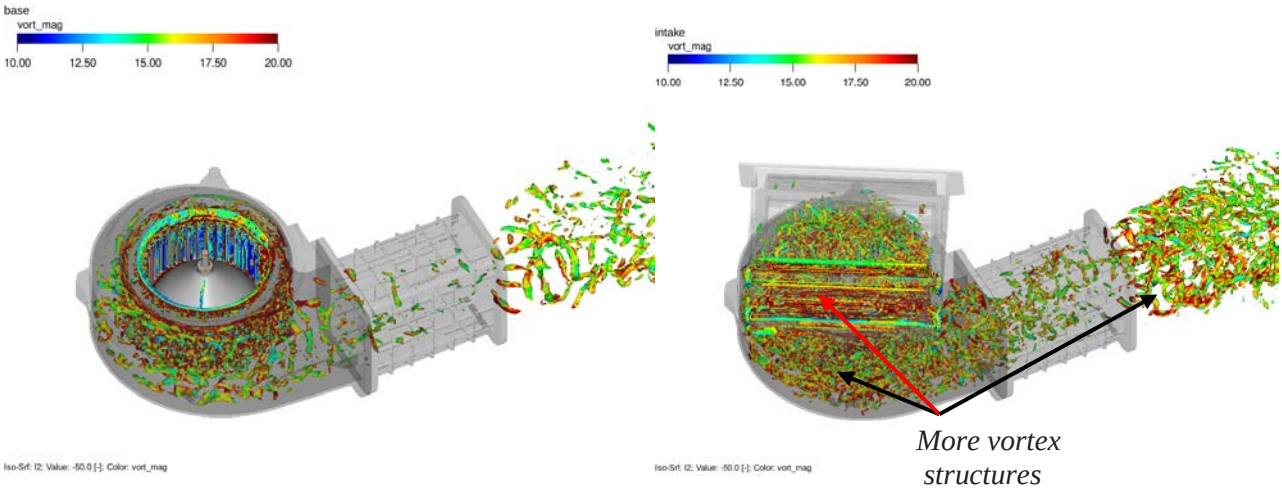

Figure 8: Instantaneous transient Lambda 2 isosurfaces (isosurface value: -50), colored by vorticity (Vorticity made dimensionless by dividing by quotient of blower tip velocity and blower diameter)

But also inside the scroll (see left black arrow in Figure 9) the vortices have increased. The air intake leads to a higher level of turbulent flow structures not only in the area close to the geometry change, but also affects downstream flow structures e.g. in the blower wheel region, the channel and at the outlet.

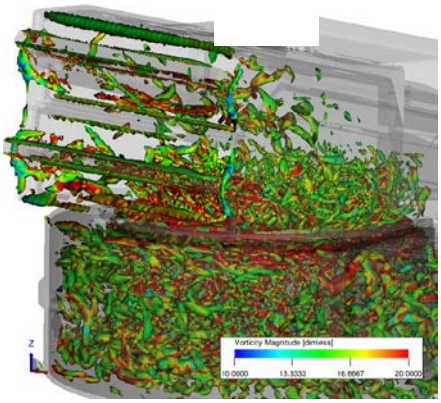

Figure 9: Instantaneous transient λ2 isosurfaces (isosurface value: -50), colored by vorticity at air intake openings

When looking at vorticity, defined as:

$$V = \nabla \times u, \tag{6}$$

, the breaking up of the flow structures is obvious (see Figure 10, right), compared to the more "smooth" vorticity structures (see Figure 10, left) the vortices have increased significantly by adding the intake.

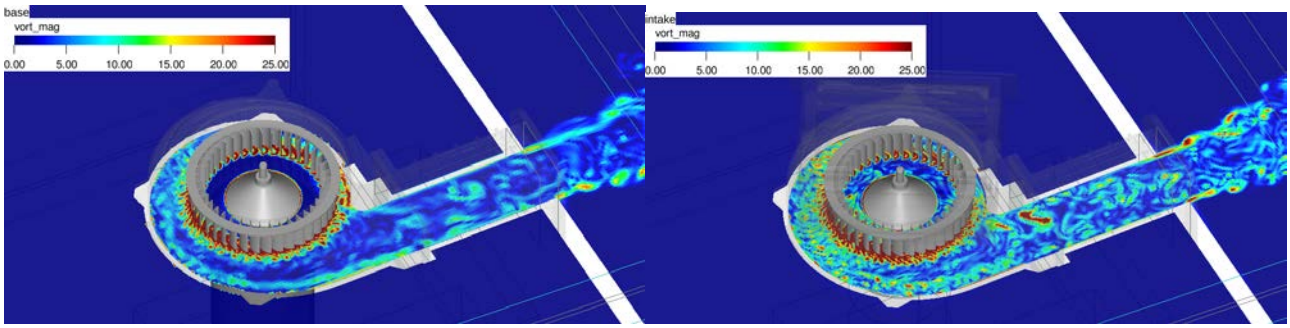

Figure 10: Instantaneous picture of transient vorticity magnitude in a plane cutting the blower wheel and chanel: with air intake: more and smaller scaled vorticity

But not only results in the time domain should be taken into account. Figure 12 beneath shows for example dBmaps on planes. To generate these, the transient pressure for each volume cell is transferred via Fast Fourier Transformation (FFT) into the frequency domain information and plotted in a dB scale, thus giving additional information about pressure fluctuations.

Higher fluctuations are observed in the "volute area" (see black arrows in Figure 11, right hand side). This corresponds well with the results illustrated in Figures 8 and 10 above.

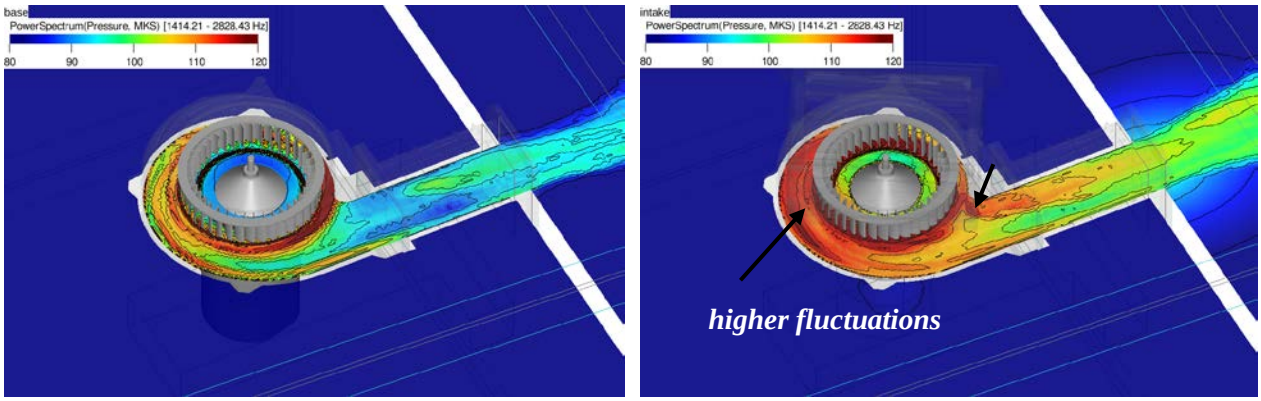

Figure 11: Octave band (2kHz) dBmaps in a plane cutting through the blower and outlet duct

dBmaps on a larger plane, extended to the exterior of the settling box, see Figure 12, give insight into the radiation behavior both inside the settling box and in the anechoic room, and show that the jet shape outside the opening is also affected by the air intake.

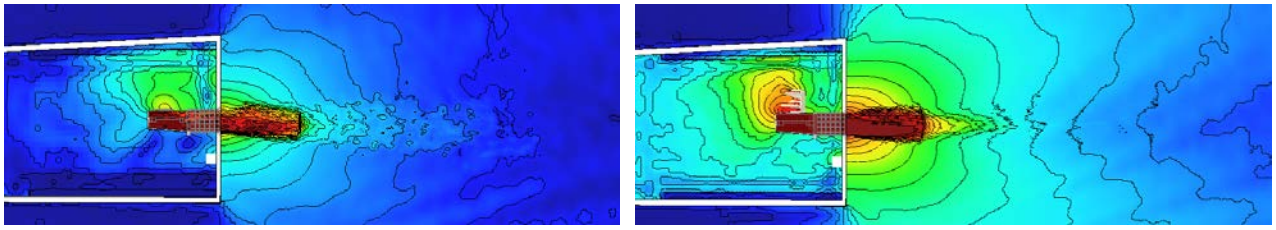

Figure 12: Octave band (2 kHz) dBmaps in a plane covering the settling box and extending into the anechoic environment. (dBmap range: 50-100dB)

A way to make acoustic waves visible is to perform an FFT (Fast Fourier Transformation), pick out a certain frequency band and transfer this back to the time domain, using inverse FFT.

An example of typical results of such procedure is given below: Figure 13 shows an instantaneous picture of band filtered pressure, demonstrating the effect of the air intake onto the radiation pattern. It must be emphasized here that both acoustic and fluid structures are visible. The hydrodynamic fluid structures, propagating with convection speed, are much smaller but show higher absolute values than the acoustic waves propagating with speed of sound.

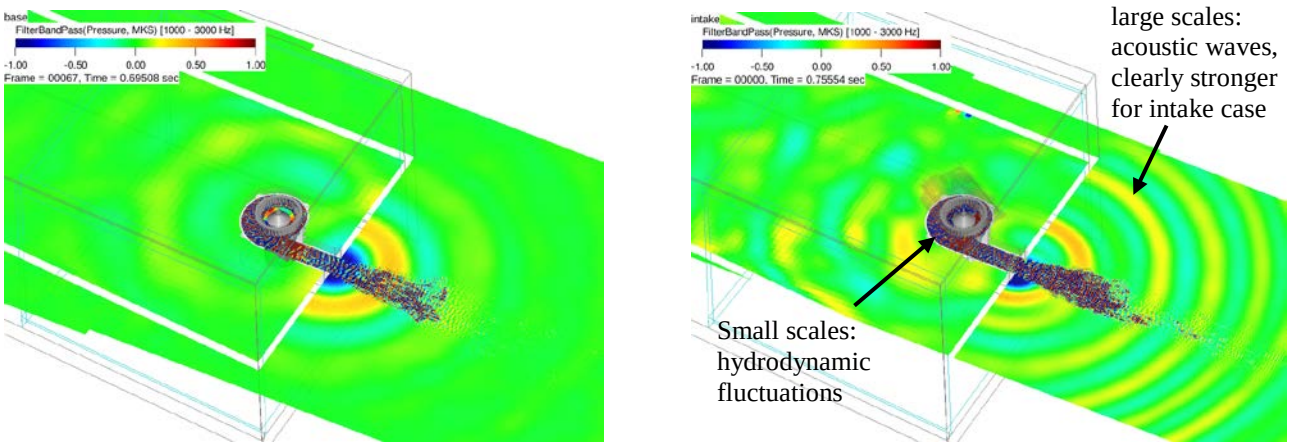

Figure13: Instantaneous band filtered pressure: 1-3 kHz; acoustic waves are visible

CONCLUSIONS

The study presented here confirms that it can be essential to take into account more realistic environments when testing the acoustics of e.g. HVAC components. Pure “laboratory conditions” allow some first insight, but are limited in terms of evaluating a system under actual operating conditions.

CFD simulation thus enables developers to test such realistic surroundings even in early project phases when the eventual mounting environment does not physically exist yet. Especially for parts like blowers, which will finally be integrated in rather complicated and constricted room conditions, this is considered to be a strong advantage.

Furthermore, transient compressible simulations like in the example presented here lead to deeper understanding of the mechanisms that generate more noise, enabling to improve a system more efficiently than by looking at integral figures only. The example shows that not only the immediate environment of the intake is affected, but that by the disturbed flow much more noise generating vortices are also generated downstream. These obviously are the reason for additional sound, which can be visualized by e.g. performing band filtering. Microphone results, verified by comparison to experiments, confirm the effect on the generated noise. In order to enhance a system acoustically, geometry changes that lead to a reduction of the significant noise generating flow structures can be virtually tested and assessed.

Finally, it should be mentioned that of course not only the acoustic behavior of systems can be evaluated, but that the Lattice-Boltzmann simulation also provides valuable information about aerodynamics and performance.

BIBLIOGRAPHY

[1] H. Chen, S. Chen, and W. H. Matthaeus – *Recovery of the Navier-Stokes equations through a lattice gas Boltzmann equation method*, Physical Review A, vol.45, 5339, **1992**

[2] H. Chen, C. Teixeira, K. Molvig – *Digital Physics Approach to Computational Fluid Dynamics, Some Theoretical Feature,* Int. J. Mod. Phys. C, 8 (4), p. 675, **1997**

[3] S. Chen, S. G. Doolen – *Lattice Boltzmann Method for Fluid Flows,* Ann. Rev.Fluid n. Mech., Vol. 30: p. 329-364, **1998.**

[4] U. Frisch, B. Hasslacher, B., Y. Pomeau – *Lattice-gas Automata for the Navier-Stokes Equation,* Phys. Rev. Lett., Vol. 56, pp.1505-1508, **1986**

[5] P. Bhatnagar, E. Gross, M. Krook – *A model for collision processes in gases. I. small amplitude processes in charged and neutral lone-component system*, Pys. Rev., vol.94, pp.511-525, **1954**

[6] S. Chapman, T. Cowling – *The Mathematical Theory of Non-Uniform Gases*, Cambridge University Press, **1990**

[7] X. Shan, H. Chen – *Lattice Boltzmann model for simulating flows with multiple phases and components*, Phys. Rev. E, 47,1815-1819, **1993**

[8] Li, Y., Shock, R., Zhang, R., and Chen, H., – *Numerical Study of Flow Past an Impulsively Started Cylinder by Lattice Boltzmann Method*, J. Fluid Mech., Vol. 519, pp. 273-300, **2004**

[9] Yakhot, V. and Orszag, S., A., 1986, – *Renormalization Group Analysis of Turbulence. I. Basic Theory*," J. Sci. Comput., Vol. 1, No. 2, pp.3-51, **1986**

[10] C. Teixeira – *Incorporating Turbulence Models into the Lattice-Boltzmann Method*, Intl. J. Mod. Phys. C, Vol. 9 No. 8, pp. 1159-1175, **1998**

[11] H. Chen, S. Orszag, I. Staroselsky, S. Succi – *Expanded Analogy between Boltzmann Kinetic Theory of Fluid and Turbulence*, J. Fluid Mech., Vol. 519, pp. 307-314, **2004**

[12] H. Chen, S. Kandasamy, S. Orszag, R. Shock, S. Succi, V. Yakhot – *Extended Boltmann Kinetic equation for Turbulent Flows*, Science, Vol.301, pp 633-636, **2003**

[13] H. Chen, C. Teixeira, K. Molvig –*Realization of Fluid Boundary Conditions via Discrete Boltzmann Dynamics*, Intl. J. Mod. Phys. C, 9 (8), p. 1281, **1998**

[14] R. Zhang, C. Sun, Y. Li, R. Satti, R. Shock, J. Hoch, H. Chen – *Lattice Boltzmann Approach for Local Reference Frames*, Commun. Comput. Phys. Vol 9 No 5, pp. 1193-1295, **2011**

[15] R. Zhang, X. Shan, H. Chen – *Efficient Kinetic Method for fluid simulation beyond Navier-Stokes equation*, Phys. Rev. E, 74, 046703, **2006**

[16] F. Perot, M.S. Kim, S. Moreau, M. Henner, D. Neal – *Direct Aeroacoustics prediction of a low speed axial fan*, AIAA 2010-3887, **2010**

[17] G. Brès, F. Pérot, D. M. Freed – *Properties of the Lattice-Boltzmann Method for Acoustics*, AIAA Paper 2009-3395, 15th AIAA/CEAS Aeroacoustics Conference, **2009**